Available online at www.sciencedirect.com
SCIENCE DIRECT®
International Journal of Solids and Structures 42 (2005) 2505–2516
INTERNATIONAL JOURNAL OF SOLIDS and STRUCTURES
www.elsevier.com/locate/ijsolstr

Experimental research on pre-cracked marble under compression

Yin-Ping Li [a,b,c,*], Long-Zhu Chen [a], Yuan-Han Wang [c]

[a] School of Civil Engineering and Mechanics, Shanghai Jiaotong University, 800 Dongchuan Road, Shanghai 200030, China
[b] Key Lab of Geomechanics, Wuhan Institute of Rock and Soil Mechanics, CAS, Wuhan 430071, China
[c] School of Civil Engineering, Huazhong University of Science and Technology, Wuhan 430074, China

Received 19 September 2004
Available online 2 November 2004

Abstract

An experimental approach on propagation and coalescence of pre-existing cracks (fractures) in marble samples under compression is carried out. Two types of newborn cracks are observed: wing (tensile) cracks and secondary (shear) cracks. Both types of cracks initiate from the tips of the fractures and propagate in a stable manner. Wing cracks initiate at an angle with the fractures and tend to propagate towards the direction of the most compressive stress. Secondary cracks, however, initiate in a direction quasi-coplanar to the fractures and also parallel to the wing cracks but in the opposite direction. The orientations and geometries of fractures can decide which kind of wing cracks and secondary cracks will be produced. The interactions between fractures strongly affect the initiation and propagation of wing cracks and secondary cracks, and make examples' failure patterns thoroughly different. The initial fracture angles of wing cracks range among 52°–68°, which are lower than the results (about 77°) of previous experiments on molding materials. In addition, the characters of acoustic emission (AE) of pre-cracked marble samples are also studied. For some rock samples, a secondary peak value phenomenon of AE counts is observed. For the samples with zigzag fractures, the accumulated AE counts at the moment of failure occupy almost half of the summation of whole load processes. This reveals that the failure of materials with zigzag fractures is more unexpected.

Keywords: Wing crack; Secondary crack; Coalescence; Acoustic emission; Marble

* Corresponding author. Address: School of Civil Engineering and Mechanics, Shanghai Jiaotong University, 800 Dongchuan Road, Shanghai 200030, China. Tel.: +86 215 471 0178; fax: +86 215 474 4255.
E-mail address: ypli@sjtu.edu.cn (Y.-P. Li).

0020-7683/$ - see front matter © 2004 Published by Elsevier Ltd.
doi:10.1016/j.ijsolstr.2004.09.033

1. Introduction

Generally, rock is a heterogeneous and anisotropic compound structure, containing many shear surfaces, cracks, weak surfaces and faultages. Failure in a rock mass can occur through sliding along persistent discontinuities, or fractures, but also through a combination of sliding along non-persistent discontinuities and bridging across unbroken rock. Extensive research has been performed on the cracking processes that occur in brittle materials in two-dimensional conditions with fractures (the term fracture will be used from now on for pre-existing cracks) through the thickness of the specimens. Reyes and Einstein (1991), Shah (1990a,b), Shen (1993, 1995), Bobet (1997), Bobet and Einstein (1998), Zhu et al. (1998), Wong and Chau (1998), Vasarhelyi and Bobet (2000) and Wong et al. (2001) have investigated crack propagation and coalescence on rock-like materials specimens containing two inclined flaws which were either both open or closed. Model materials can simulate well some characteristics of real rock, for example, brittleness and shear-dilatability, however, it is difficult to simulate all characteristics of real rock materials with abundant meso-structures. So, besides model materials, real rock samples are also employed to study rock materials with fractures. Examples include the work of Ingraffea and Heuze (1980) on limestone, Petit and Barquins (1988) on sandstone, Jiefan et al. (1990) and Chen et al. (1992) on marble, Huang et al. (1999) and Celestino et al. (2001) on marble and Shang et al. (1999) on granite and marble. However, in these studies on real materials, the rock samples were usually made to be thin slices with some slots for the purpose of scanning electron microscope (SEM) study.

A common crack pattern found in rocks and rock-model materials in compression was summarized by Bobet (2000) as follows (see Fig. 1): 1. Wing cracks start at the tips of the fractures and propagate in a curvilinear path as the load increases. Wing cracks are tensile cracks, and they grow in a stable manner, since an increase in load is necessary to lengthen the cracks. Wing cracks tend to align with the direction of the most compressive stress. 2. Secondary cracks are generally described as shear cracks or shear zones. They initiate from the tips of the fractures; two directions are possible: (1) coplanar or nearly coplanar to the fractures; (2) with an inclination similar to the wing cracks but in the opposite direction.

It should be noted that the two initiation directions of the secondary crack are not observed in all experiments. The quasi-coplanar direction has been systematically observed in a large number of tests, while the second one only in few tests. For instance, Ingraffea and Heuze, Petit and Barquins, Reyes, Shen, Bobet, Bobet and Einstein, and Wong and Chau only observed secondary cracks in the direction coplanar to the

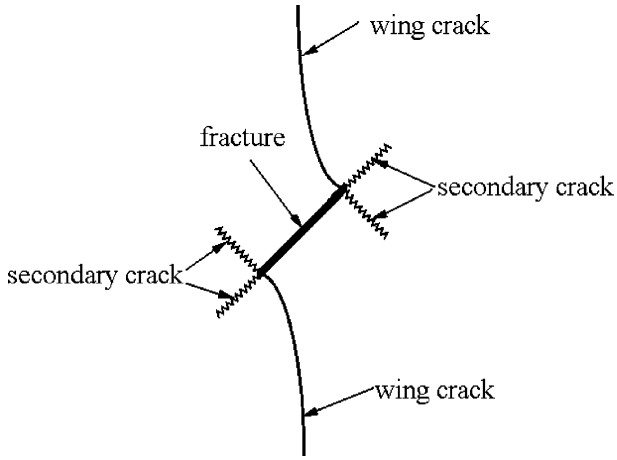

Fig. 1. Simplified crack pattern in pre-cracked specimens of rock materials in uniaxial compression (Bobet, 2000).

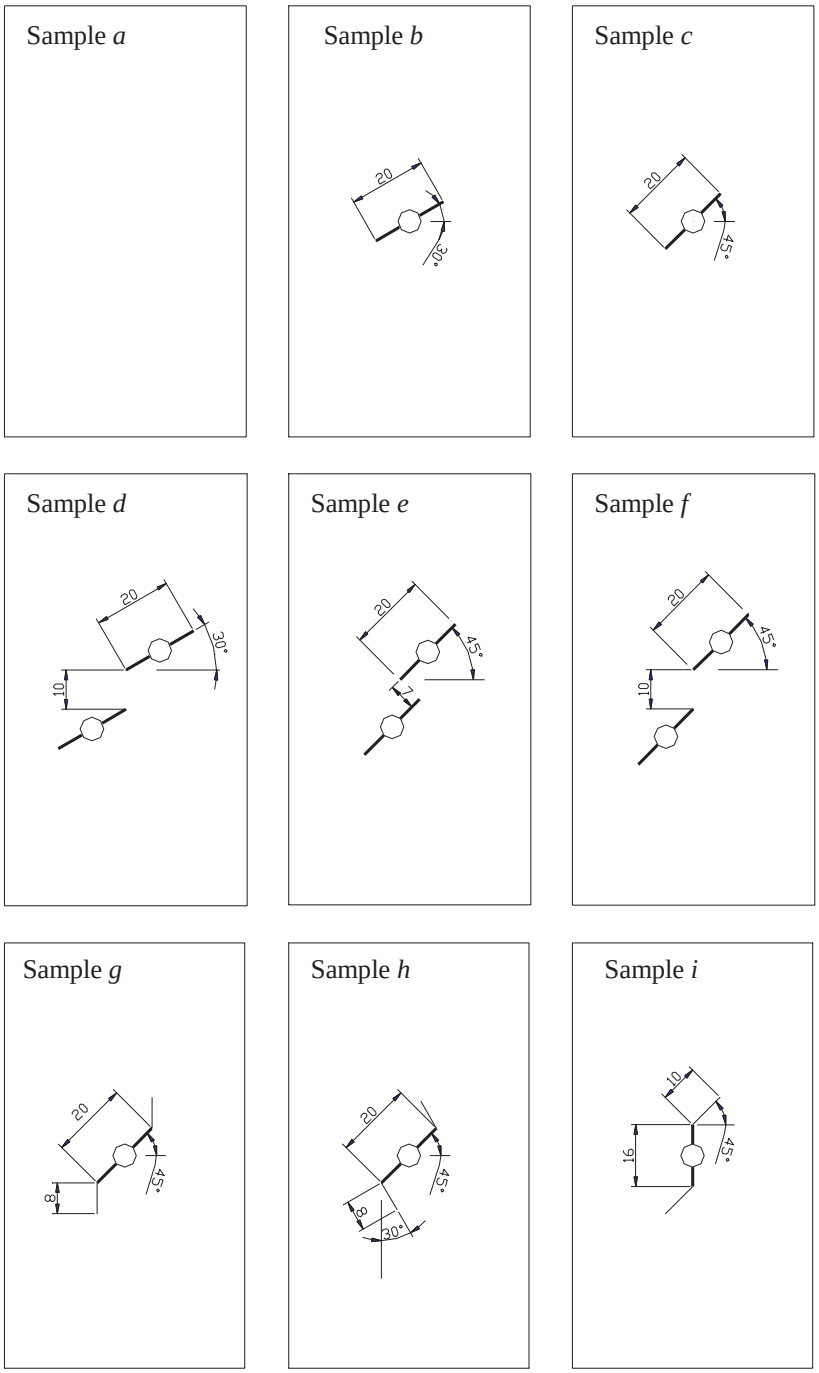

Fig. 2. Dimensions of samples.

fractures. Thus, it may be argued that the direction of initiation of the secondary cracks may be material dependent. An extension of the conventional maximum tangential stress criterion was proposed by Bobet (2000), in which the direction and stress level of shear crack initiation are determined by the direction and magnitude of maximum shear.

Therefore, it becomes a worthwhile and interesting question whether one can discover all two types of secondary crack in a set of test, by variation of the number, the geometries or even the shapes of fractures. In addition, in most of the above researches, the fractures in rock were usually simulated by one or two more inclined straight cracks. Actually, taking 2D case for example, Li and Wang (2003) pointed out that the shapes of the persistent cracks in natural rock may be various, e.g., cross line, irregular curve and polygonal (zigzag) line as well as straight line.

An experimental approach on marble samples, which have similar outline dimensions as model rock specimens in previous studies and include various shape cracks, is presented to study initiation of wing cracks and secondary cracks and coalescence of fractures under compression in this paper.

2. Preparation of marble samples

The experiment material is marble of Huangshi, Hubei Province, China, provided by Wuhan Institute of Rock and Soil Mechanics, CAS. The outline dimensions of samples are uniform (110 mm × 62 mm × 25 mm) but with different internal crack dimensions. According to the differences of shapes and number of fractures, these samples were divided into four kinds: (1) perfect samples (a); (2) samples with single fracture (b–c); (3) samples with a pair of parallel fractures (d–f); (4) samples with zigzag cracks (g–i).

The lengths, inclined angles and rock bridge dimensions of cracks are illustrated in Fig. 2. It is somewhat difficult to cut flaws in the thick specimens of real rock. However, for similar materials, it can be done easily by inserting steel or copper slices during molding process. The samples were prepared in the center of sample machining of Optics Department, Huazhong University of Science and Technology. After several discussions, a plan was decided eventually, in which holes would be drilled before the fractures were cut artificially. There were three steps of the same procedure:

(1) cutting and burnishing the rude marble mass, ensuring the accuracy of dimensions and the parallel of two load surfaces;
(2) drilling holes of 6 mm diameters (for the sample thickness was 25 mm, considering stiffness of the drill, the diameter of drill could not be too small);
(3) cutting cracks artificially.

The last step, sawing back and forth along the fractures' directions by emery steel thread, was time-consuming. The thickness of cracks, 0.5–1 mm, was not fairly small. Obviously, the presence of the machining holes will affect the stress and strain fields near crack tips, but its influence was proved to be finite by the following FEM analysis (see Section 5).

3. Testing equipment

The test was performed using an HT-9501 servo material test machine in the Civil Department, Huazhong University of Science and Technology. This machine can record load-displacement curves and computer the elastic modulus automatically. At the same time, an AE21C-04 Acoustic Emission System was adopted to detect damage and fracture of rock samples, and a Digital Camera was used to record the cases of crack initiation, crack propagation and failure patterns of the specimens.

4. Experiment results and analysis

4.1. Wing cracks, secondary cracks and failure patterns

This test adopted equal strain rate loading, and the loading rate was 0.2%/min. Under uniaxial compression, the basic characteristic of crack propagation was that wing cracks and secondary cracks usually initiated from tips of the fractures. Similar to crazes in Polymer materials, the newborn cracks behaved as a narrow white belt at the beginning, which indicated deviation and failure of crystalline grains in marble. The white area expanded continuously and its color became deeper. Eventually, the propagation and coalescence of cracks resulted in unstably collapse of samples. The destroyed samples (e.g., specimen c in Fig. 3) showed that there were two kinds of macro newborn cracks, one for tensile wing cracks with neat faces, and the other for compression shear secondary cracks with crude sawtooth faces.

Sample b contained only one fracture as well as sample c, but the inclinations of their fractures were different (one at 30° and the other at 45° with horizontal line). It was found that the directions of fractures strongly affect the mechanical properties of the samples. As shown in Fig. 4, for sample b, the wing crack initiated earlier along the direction of the principal compression stress. The initial fracture angle was 66°, and the sample fractured quickly. On the other hand, for sample c, besides the initiation and propagation of wing crack, the secondary cracks in a direction quasi-coplanar to the fractures, were also observed. Whole collapse of the specimen was due to the development of the secondary cracks. The wing cracks were regular while the secondary cracks were fairly rough, similar to a fragmentized band.

Both sample d and sample f contained two offset parallel fractures, but their fracture inclined angles were different. It was also indicated that the influences of crack directions were obvious. For sample d, only the initiation and propagation of wing cracks were observed, and two fractures coalesced by a straight line, which indicated a tension model fracture. At the other tips of cracks, the wing cracks split the sample vertically, and no secondary crack was observed. For sample f, the cases of tips were considerable complicated. Two types of cracks, wing cracks and secondary cracks, as shown in Fig. 4, initiated from the fracture tips, and the secondary cracks bifurcated and then produced a crack along the loading direction. The new bifurcated crack eventually resulted in the final failure. In rock bridge region, wing cracks were also initiated too, but propagated slowly. Although they coalesced too before whole collapse, the coalescence crack was not as neat as that of sample d. This revealed the coalescence of sample f was tension-shear-mixed model.

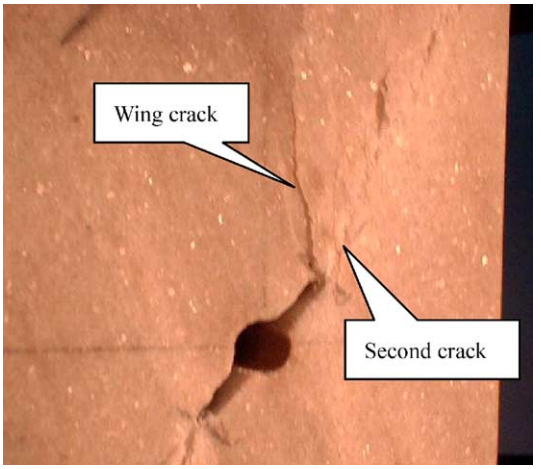

Fig. 3. Two kinds of new born cracks.

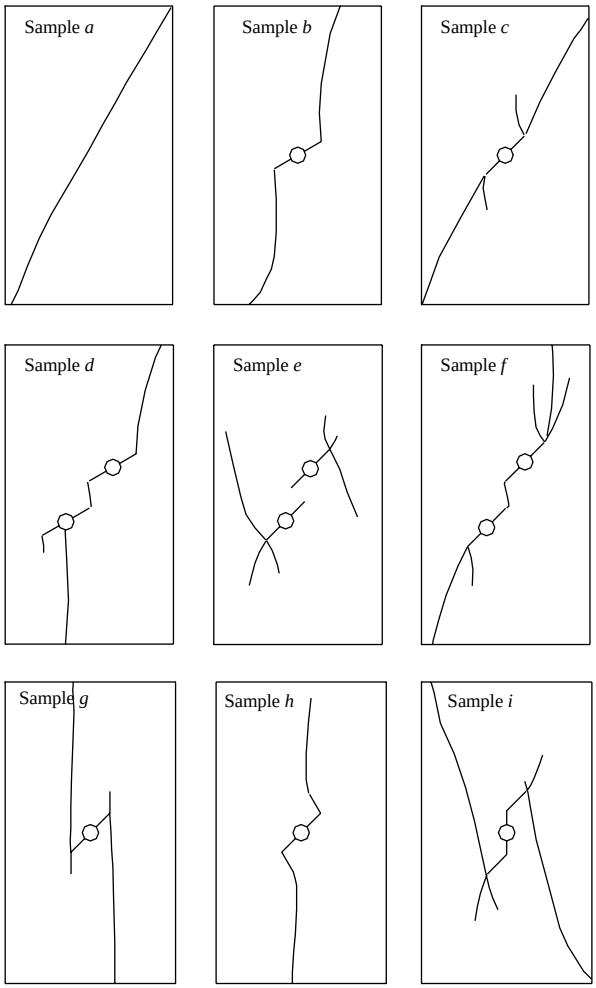

Fig. 4. Failure patterns of samples.

The lengths and inclinations of the fractures in sample e and sample f were the same, but the dimensions of rock bridge regions were different. Compared with sample e, the two fractures in sample f looked like move towards each other along the fracture inclination. From experiment results, one know that the critical failure load of sample e was lower than that of sample f. In rock bridge region, due to the stress shielding, two crack tips produced no wing cracks or secondary cracks and hardly coalesced until whole collapse of the sample. Wing cracks initiated from the outer crack tips and then the secondary cracks (parallel to the wing cracks but in opposite direction) were produced. It was the propagation of the opposite secondary cracks that resulted in the final failure of sample e.

Especially, zigzag cracks were pre-existing in samples g, h and i. Zigzag Crack Model were proposed first and analyzed theoretically by Li and Wang (2003). This model is an expansion of Sliding Crack Model. A primary experimental approach on this model was achieved here. It was shown that the inclinations and geometries of zigzag fractures were of obvious influences on the properties of specimens. As shown in Fig. 4, for sample g, its pre-existing wing cracks (kinks) along loading direction did not propagate further at all. There were new secondary cracks that initiated along the opposite direction of the pre-existing kinks,

Table 1
Initial fracture angles, elastic moduli and critical collapse loads

Sample number	Initial angles	Elastic moduli (GPa)	Critical collapse loads (MPa)	Supplement
a	–	16.5	77.35	No crack
b	66°	12.9	45.02	Single crack
c	55°	15.1	61.79	Single crack
d	63°	10.1	33.29	Double cracks
e	52°	14.8	40.65	Double cracks
f	58°	14.5	47.32	Double cracks
g	–	11.0	43.93	Zigzag crack
h[a]	–	–	–	Zigzag crack
i	56°	13.3	57.73	Zigzag crack

[a] For sample h, the machine did not record the elastic modulus and the critical collapse load correctly.

and eventually induced the final fracture of specimens. However, for sample h, in which the pre-existing kink made a 75° angle with the main fracture, the kinks expanded further and aligned gradually itself along the direction of load. This showed that the angles made by the kinks and the main fractures affected strongly propagation and coalescence of zigzag fractures. For sample i, in which the kink made a 45° angle with the main fracture, its failure patterns were more complicated. Both new kinks and secondary cracks quasi-coplanar to the fractures initiated, and then the opposite secondary cracks of the new kinks were produced. So, two types of secondary cracks were produced in the same specimen with zigzag fracture. It is the secondary cracks (in the opposite direction of the kink) that resulted in the final collapse of samples. The pre-existing wing cracks were almost closed after failure.

From mentioned above, one know that: for samples with single fracture, secondary cracks opposite to the wing cracks were not observed; for some case of overlapping geometries that the fractures overlap extraordinarily in the direction of loading (i.e., in sample e), secondary cracks opposite to wing cracks follow immediately after wing cracks initiate; for samples with zigzag fractures, i.e., samples g and i, failure is usually produced by the initiation and propagation of secondary cracks. The initiation of a tensile kink relieves the tensile stresses around the tip but the singularity of the shear stresses at the tip of the fracture may still exist. One may hypothesize that the shear stress singularity could be responsible for the initiation of the

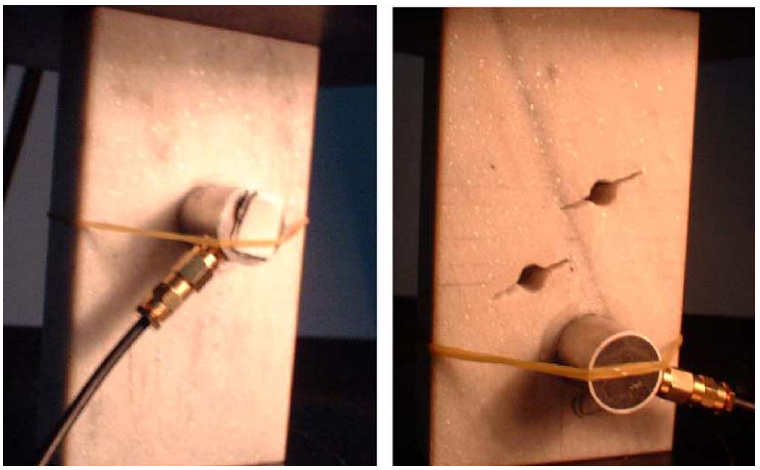

Fig. 5. Samples (a and d) with AE sensors.

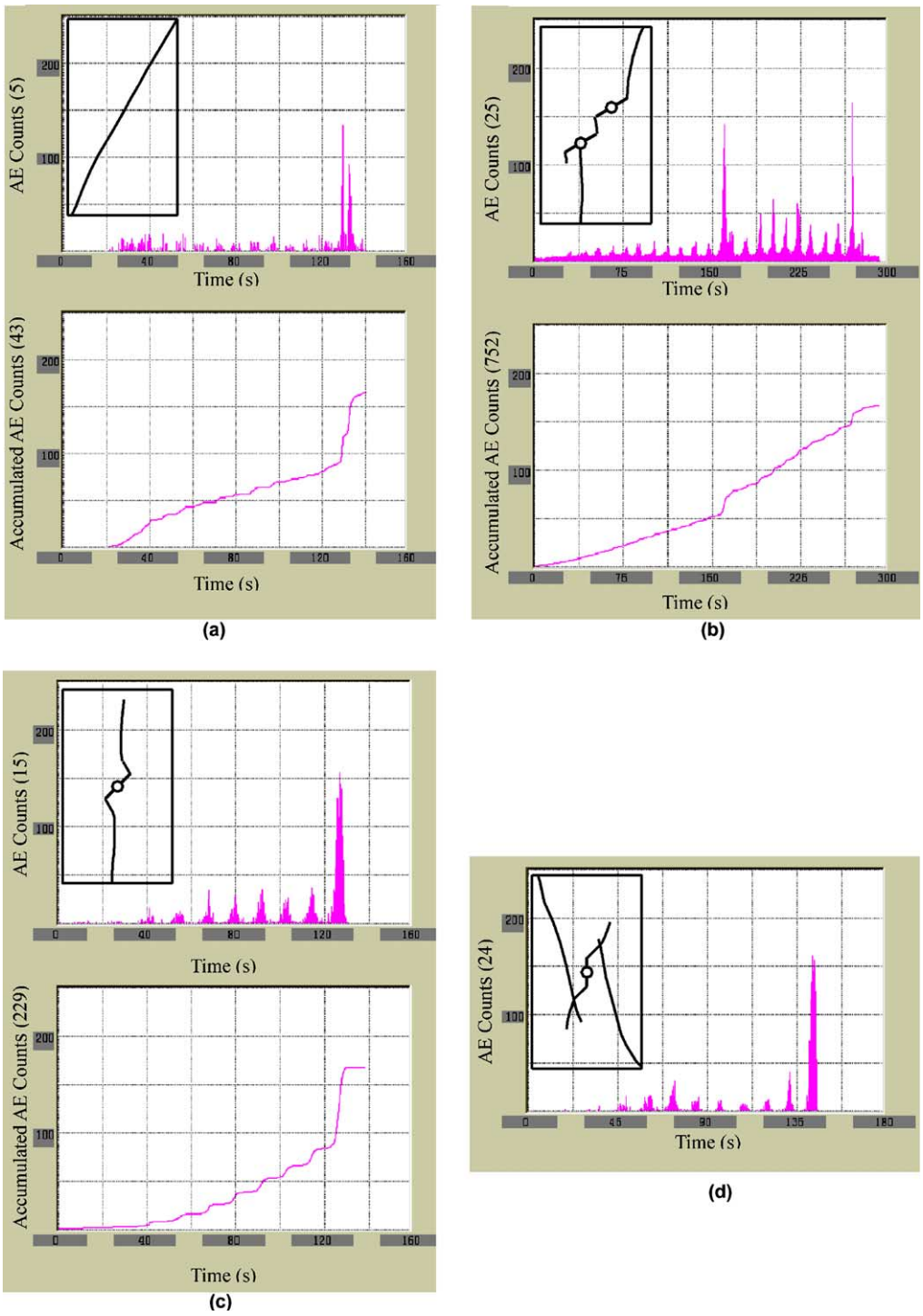

Fig. 6. AE counts and accumulated AE counts of samples: (a) sample a; (b) sample d; (c) sample h; (d) sample i (AE counts only). The numbers in double bracket in vertical axis labels are the multiplier of coordinates.

secondary shear crack. Further investigation on stresses around the tips of a fracture with a kink should be conducted to explore this possibility.

4.2. Initial fracture angles and critical collapse loads

The initial fracture angles, elastic moduli and critical collapse loads, etc. are listed in Table 1. The initial fracture angles of wing cracks in marble ranged among 52°–68°, which were lower than the results (about 77° of previous experiments (Zhu et al., 1998) on similar molding materials. This indicated that the molding materials couldn't simulate fully the characters of the real rock materials. The elastic moduli of the perfect samples were about 16.5 GPa, but the elastic moduli of the samples with fractures were all reduced.

4.3. AE characters of marble samples

Under the action of load, damage will be produced in rock-like materials. The deformation and failure phenomenon in materials is the macro representation of the micro or meso distortion and fracture. AE, an efficient tool to detect inner distortion in rock materials, can reflect the evolvement and propagation of defects in materials. As illustrated in Fig. 5, AE sensors were stuck on the marble samples using vaseline and fixed slightly by elastic bands. The AE counts and the accumulated AE counts were recorded on line by the AE21C-04 Acoustic Emission System.

The relationship curves of AE counts vs. time and accumulated AE counts vs. time of part samples are shown in Fig. 6. Actually, for equal strain rate loading, time is proportional to the total strain. The AE characters of different samples indicated that their failure mechanisms were distinguishing.

The AE counts and accumulated AE counts of the perfect sample a are shown in Fig. 6(a). AE signals were fairly steady and not active before whole failure of samples. However, at the moment of failure process, the accumulated AE counts reached a peak value.

As shown in Fig. 6(b), the AE counts of sample d had two peak values, and the accumulated AE counts had two steep slopes accordingly. The first steep slope corresponded to the beginning of initiation of wing cracks and secondary cracks from fracture tips; the second one indicated the whole collapse of samples. So, AE signals reflected successfully the staggered processes of failure.

The AE counts of samples h and i with zigzag cracks were shown in Fig. 6(c) and (d). Similar to perfect samples, a peak value of AE counts was presented. AE signals in these samples, however, different from that of other samples, were quite active. It is shown that the accumulated AE counts at the moment of failure occupied almost half of summation of whole process. This reveals that the failure of materials with zigzag fractures is more unexpected and unpredictable, and deserved to be studied further.

5. Numerical investigation of the influence of machining holes

Before the numerical simulations are discussed, the essential features of RFPA^{2D} code are summarized briefly in this section. The RFPA^{2D} is a progressive elastic damage model; it can be used to simulate the deformation, stress distribution and failure induced stress redistribution, fracture initiation and fracture propagation in heterogeneous materials. The consideration of heterogeneity for the elements is achieved by assigning the elements random strength and elastic modulus by assuming a Weibull's distribution. Although fracture mechanics plays an important role in the analysis of crack propagation, the assumption of homogeneity adopted in fracture mechanics limits its application in heterogeneous materials. Instead of using a fracture mechanics approach where fracture propagation is related to a stress intensity factor at the advancing crack tips and is controlled by the fracture toughness, a failure approach is adopted in the code,

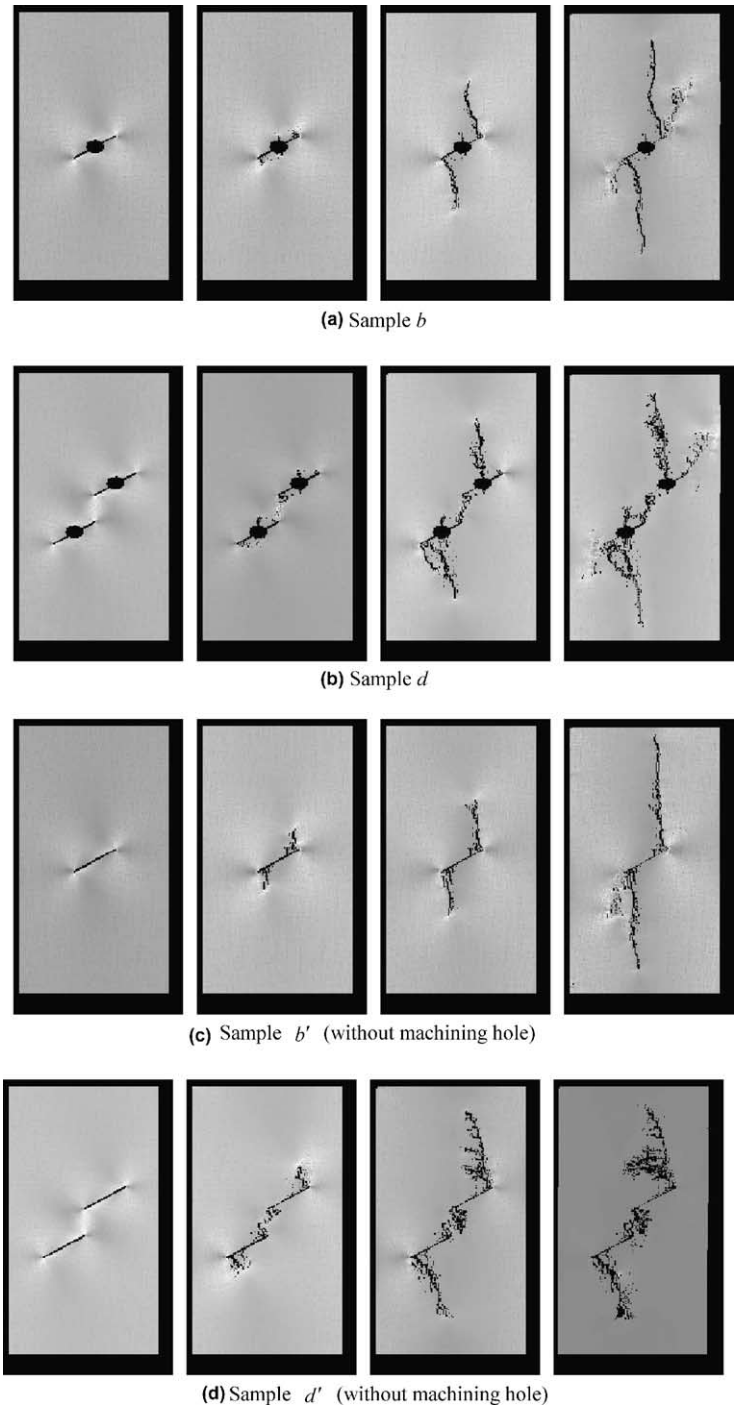

Fig. 7. Numerical simulation of samples' failure process (a) sample b; (b) sample d; (c) sample b′ (without machining hole); (d) sample d′ (without machining hole).

RFPA^{2D}, where microfracturing occurs when the stress of an element satisfies a certain strength criterion (Tang and Kou, 1998).

In this investigation, a Coulomb criterion envelope with a tensile cut-off is used so that the elements may fail either in shear or in tension. The element property is selected by setting the Weibull's distribution (m; s_0 as E_0 (5, 16.5 GPa) and σ_0 (5, 70 MPa). The parameter m is a homogeneity index which controls the shape of the distribution function with respect to the degree of material heterogeneity; s_0 is the parameter related to the mean value of the material parameters for the elements, such as compressive strength σ_0 and elastic modulus E_0. The residual strength coefficient λ is supposed to be 0.1. The Poisson's ratio is 0.25. The ratio of tensile strength to compressive strength and the average friction angle for the elements are 1/8 and 30°, respectively.

The simulation proceeds as follows: an external displacement with a constant rate is applied in the vertical direction to produce a compression loading to the sample. No end friction is induced between the specimen and loading platen. The stress and deformation distribution in the sample is calculated in steps.

Samples b and d were taken as test examples to analyze the influence on failure patterns of presence of the machining holes. As shown in Fig. 7(a) and (b) respectively, the gradual damage and failure processes of samples b (with a fracture inclining angle), 30°and d (with a fracture inclining angle), 45°were simulated by using RFPA^{2D}. Comparing the numerical results of failure patterns (Fig. 7(a) and (b)) and experimental ones (samples b and d in Fig. 4), one can know that the FEM analysis got a good simulation of the experimental processes. Under uniaxial compression, the basic characteristic of crack propagation was that wing cracks and secondary cracks usually initiated from tips of the fractures. This is coincident with the analytic results of classical fracture mechanics.

For investigating the influence of the presence of the machining holes, the virtual samples b′ and d′, with same materials, dimensions and fractures of samples b and d but without the machining holes, were also analyzed. The numerical results are illustrated in Fig. 7(c) and (d). By comparing the failure patterns of samples b and d with the ones of samples b′ and d′, one can find that, the presence of the machining holes affects the properties of the samples weakly. Although it may make the initial fracture angles get a little bigger and promote slightly the initiation of secondary cracks rather than wing cracks, it does not impose essential affection on the damage and failure of the samples. So, the results on the samples with machining holes are reliable.

In addition, the shear stress fields are also presented by brightness ranging from very dim to very bright: the brighter the area is, the stronger the shear stress is. One can know that the shear stress concentrates extraordinarily near the tips of pre-existing fractures and newborn cracks.

6. Conclusions

An experimental approach on the propagation and coalescence of fractures in marble samples under compression was carried out. Some conclusions could be drawn as followings:

(1) In the test on marble materials, two types of newborn cracks are observed: wing (tensile) cracks and secondary (shear) cracks. Both types of cracks initiate from the tips of the fractures and propagate in a stable manner. Wing cracks initiate at an angle with the fracture and tend to propagate towards the direction of the most compressive stress. Secondary cracks, however, initiate in a direction coplanar or quasi-coplanar to the fractures and also parallel to the wing cracks but in the opposite direction. The orientations and geometries of fractures can decide which kind of wing cracks and secondary cracks will be produced. In the samples with overlapping geometries fractures or zigzag fractures, secondary cracks in the opposite direction of wing cracks were produced.

(2) The initial fracture angles of wing cracks in marble range among 52°–68°, which are lower than the previous results of experiments on molding materials. This indicates that there are considerable differences between marble and molding materials.
(3) For the samples with zigzag fractures, the failure mechanism is more complicated. As the sample whole collapses, AE counts reaches a peak value and the accumulated AE counts of failure process occupies almost half of the summation of whole load processes. This reveals that the failure of materials with zigzag fractures is more unexpected and unpredictable.
(4) The acoustic emission of the whole processes can be divided to be three stages: elastic stage, crack initiation stage and failure stages. For some marble samples, in which the damage is due to the initiation and propagation of wing cracks or secondary cracks and the final failure of samples is produced by the coalescence of fractures, a double peak value phenomenon is observed. This may provide a useful reference for the detection of rock mass stabilization.

References

Bobet, A., 1997. Fracture coalescence in rock materials: experimental observations and numerical predictions. Sc.D. Thesis, MIT, Cambridge, USA.
Bobet, A., 2000. The initiation of secondary cracks in compression. Eng. Fract. Mech. 66, 187–219.
Bobet, A., Einstein, H.H., 1998. Fracture coalescence in rock-type materials under uniaxial and biaxial compression. Int. J. Rock Mech. Min. Sci. 35, 863–889.
Celestino, S.P., Piltner, R., Monteiro, P.J.M., Ostertag, C.P., 2001. Fracture mechanics of marble using a splitting tension test. J. Mater. Civ. Eng. 13, 407–411.
Chen, G., Kemeny, J., Harpalani, S., 1992. Fracture propagation and coalescence in marble plates with pre-cut notches under compression. Symp. on Fractured and Jointed Rock Mass, Lake Tahoe, CA, pp. 443–448.
Huang, M.L., Tang, C.A., Zhu, W.C., 1999. Real-time SEM study on rock failure instability under uniaxial compression. J. North Univ. (Nat. Sci.) 20, 426–429 (in Chinese).
Ingraffea, A.R., Heuze, F.E., 1980. Finite element models for rock fracture mechanics. Int. J. Numer. Anal. Meth. Geomech. 4, 25–43.
Jiefan, H., Ganglin, C., Yonghong, Z., Ren, W., 1990. An experimental study of the strain field development prior to failure of a marble plate under compression. Tectonophysics 175, 269–284.
Li, Y.P., Wang, Y.H., 2003. Analysis on zigzag cracks in rock-like materials under compression. Acta Mech. Solida Sinica 24, 456–462, in Chinese.
Petit, J., Barquins, M., 1988. Can natural faults propagate under mode II conditions?. Tectonics 7, 1243–1256.
Reyes, O., Einstein, H.H., 1991. Failure mechanism of fractured rock—a fracture coalescence model. In: Proc. 7th Congress of the ISRM, Tokyo, Japan, 1, pp. 333–340.
Shah, S.P., 1990a. Fracture toughness for high-strength concrete. ACI Mater. J. 87, 260–265.
Shah, S.P., 1990b. Experimental methods for determining fracture process zone and fracture parameters. Eng. Fract. Mech. 35, 3–14.
Shang, J.L., Kong, C.J., Li, T.J., Zhang, W.Y., 1999. Observation and study on meso-damage and fracture of rock. J. Exp. Mech. 14, 373–383, in Chinese.
Shen, B., 1993. The mechanics of fracture coalescence in compression experimental study and numerical simulation. Eng. Fract. Mech. 51, 73–85.
Shen, B., Stephansson, O., Einstein, H.H., Ghahreman, B., 1995. Coalescence of fracture under shear stresses in experiments. J. Geophys. Res. 100, 725–729.
Tang, C.A., Kou, S.Q., 1998. Fracture propagation and coalescence in brittle materials. Eng. Fract. Mech. 61, 311–324.
Vasarhelyi, B., Bobet, A., 2000. Modeling of crack initiation, propagation and coalescence in uniaxial compression. Rock Mech. Rock Eng. 33, 119–139.
Wong, R.H.C., Chau, K.T., 1998. Crack coalescence in a rock-like material containing two cracks. Int. J. Rock Mech. Min. Sci. 35, 147–164.
Wong, R.H.C., Chau, K.T., Tang, C.A., Lin, P., 2001. Analysis of crack coalescence in rock-part I: experimental approach. Int. J. Rock Mech. Min. Sci. 38, 909–924.
Zhu, W.S., Chen, W.Z., Shen, J., 1998. Simulation experiment and fracture mechanism study on propagation of Echelon pattern cracks. Acta Mech. Solida Sinica 19, 355–360, in Chinese.